

# Implementation of Control Unit for Electric Drive Kart

Ondřej Suchý

Department of Electromechanics and Power  
Electronics  
University of West Bohemia  
Pilsen, Czech Republic  
suchyo@rice.zcu.cz

Tomáš Košan, Luboš Streit

Regional Innovation Centre for Electrical  
Engineering  
University of West Bohemia  
Pilsen, Czech Republic  
kosan@rice.zcu.cz, lloyd@rice.zcu.cz

**Abstract** – This paper presents the design of the control unit to be installed in the electric kart and it will control the permanent magnet synchronous motor as well as other peripherals. The control unit contains microcontroller TMS320F28335, analog circuits for voltage and current sensors, drivers for 3-phase inverter, CAN and RS-485 communications and circuit for power outputs.

**Keywords** - Permanent magnet synchronous motor; TMS320F28335; field-oriented control; position sensor; drivers for power transistors; 3-phase inverter; go-kart

## I. INTRODUCTION

This paper deals with realization of control unit, which will control synchronous motor with permanent magnets, resp. BLDC with sinusoidal induced voltage. This compact unit (converter integrated with the control unit into a single assembly) will be mounted on the electric go-kart used by the Department of Electromechanics and Power Electronics (KEV) for promotional purposes. In these papers [1] and [2], there are similar projects focused on electric go-karts. Up to date go-kart has been fitted with a step-down converter only, which does not allow recuperative braking. Control was realized by Atmel AVR microcontroller with 16MHz clock frequency only. The present electric kart is fitted with a permanent magnet DC motor with a power of 5kW. Information about the electric go-kart are written [3].

The replacement of the existing solution should achieve the same performance, but with less weight and higher efficiency. The original control did not allow recuperation to the batteries which is now possible with the current topology. Another new feature is the ability to communicate with the kart display through CAN bus as well as with balancers connected to batteries. The compact drive block with control unit is also designed for high splash resistance. It is mounted in a box which is completely sealed against splash water. For this purpose, were selected connectors with at least IPx4 protection and this requirement was already considered during the design.

## II. DESIGN OF CONTROL UNIT

Requirements for control unit was defined by used PMSM, control method and connected peripherals like front and rear lights etc.

Main requirement was a galvanic insulation of the board from the battery pack. The motor control demands current and dc-link voltage measurements together with rotor position. Control unit is also responsible for charging of battery pack. CAN and RS-485 are needed for communication with display and balancers which control batteries. The last important parts are measurement of the throttle and brake pedals. Figure 1 shows the block diagram of the individual function blocks and their interconnection with other units. The control unit operates with an input voltage range from 35 V to 65 V (nominal voltage of batteries is 48V). Main supply for control unit is main battery pack. This voltage is converted to 12V with insulated step-down converter with maximal current of 5A. All other voltages (5, 3.3 and 1.9V) are provided by another set of non-insulated step-down converters.

All controls and measurements are implemented in the TMS320F28335 microcontroller, which was selected with regard to a sufficient number of I / O pins, PWM outputs and A / D converter inputs.

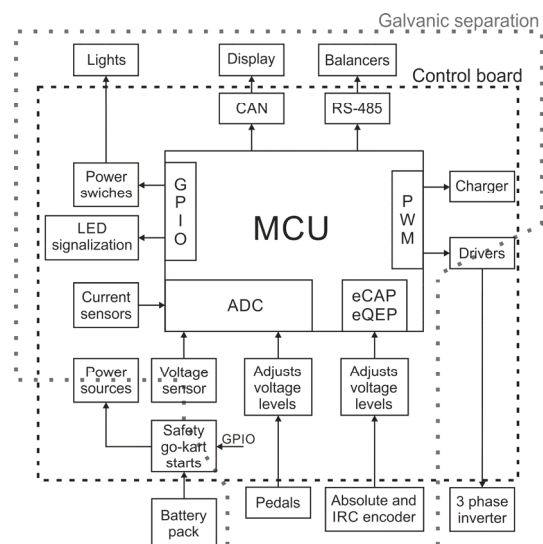


Figure 1. Block diagram for control board with peripherals

### A. Microcontroller

TMS320F28335 from Texas Instruments is a 32-bit CPU that has static CMOS technology. This microcontroller is optimized for real-time control applications such as motor drivers, electric vehicles and

transportation. Block diagram for TMS320F28335 is in Figure 2. It has these parameters [4]:

- Power 1.9V core, 3.3V I / O pins
- Core clock frequency up to 150MHz
- Memory 256K x 16 Flash, 34K x 16 SARAM
- 18 PWM outputs, 6 HRPWM outputs, 6 event capture inputs
- 8x 32-bit timers (6 for eCAP and 2 for eQEP)
- 9x 16-bit timers (6 for ePWM and 3 for XINTCTR)
- 12-bit ADC, 16 channels (2x8), 2x sample / hold units, range 0 - 3V
- 88 multiplexed GPIO pins with input filter
- 2x CAN, 3x SCI, 2x McBSP, SPI, I2C

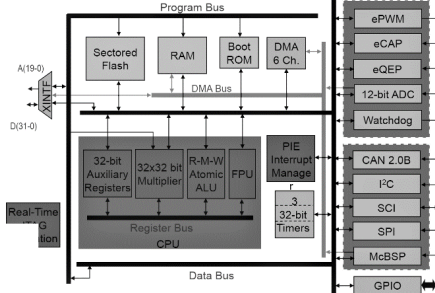


Figure 2. Block diagram of TMS320F28335 [4]

### B. Safety go-kart starts

The main battery pack uses four 12V LiFeYPO4 batteries which are sensitive to deep discharge, therefore special protection circuit is placed on power supply input of control unit. The block diagram for safety go-kart starts is shown in Figure 3.

Until the key is turned on, the entire kart is disconnected from the battery. When the key is turned on, the power is connected to the control board, where the input voltage is analyzed by the voltage sensor and according to this information, is decided about the power supply status (stay connected or to be disconnected).

The safety go-kart start circuit ensure that the control unit will be forcibly disconnected from the battery when it has insufficient voltage. The battery is thus protected against being deeply discharged. The battery powers the step-down converter with a very low idle current, which provides power for the TLC555 [5]. The TLC555 is connected as a delayed trip circuit. It means that as soon as voltage on the power terminals is sufficiently high the output is immediately switched on and will remain on the set 3 seconds. After this time, the control unit power is disconnected. During this time, the microcontroller must boot-up and measure voltage of battery. If measured value indicates sufficient voltage for go-kart operation then MCU bypasses protection circuit. From now and then MCU is responsible for battery protection.

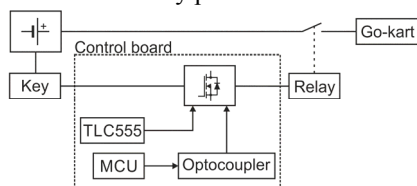


Figure 3. Block diagram for safety go-kart start

### C. Rotor position determination

Field-oriented control needs to know the exact position of the rotor for proper PMSM control. The PMSM motor can also be controlled without the encoder. This issue is addressed in papers [6] and [7]. Measured rotor position is used by Park Transform to convert currents from static reference frame to rotating reference frame d, q. A high reliability of motor control is required thus sensorless methods were not used and rotor position is measured by absolute position encoder.

An AS5040 [8] sensor is used where combination of PWM encoded absolute position and incremental pulses are used to obtain current rotor position. Combination of these two methods eliminates lag of PWM output of sensor which is about 1 ms as it is almost unusable for proper control of PMSM.

The sensor has 6 Hall sensors in a circle, from which is evaluated the angle of rotation of the rotor shaft. For the measurement it was necessary to mount a diametric magnetized magnet on the motor shaft. This creates a magnetic field which is sensed by the Hall probes integrated DSP core then process measured fields and calculate position of the rotor. The sensor can measure the rotor angle with a resolution of  $0.35^\circ$  at speeds up to 30000rpm.

## III. FIELD ORIENTED CONTROL

Field-oriented control for PMSM consists of three larger parts, which are: 1) controllers, 2) transformations and 3) PWM modulator, block diagram is shown in Figure 4. For control of go-kart is used the simplest type of field-oriented control, which does not have implemented feed-forward model of motor. More complex types of field-oriented control can be found in the papers [9], [10] and [11].

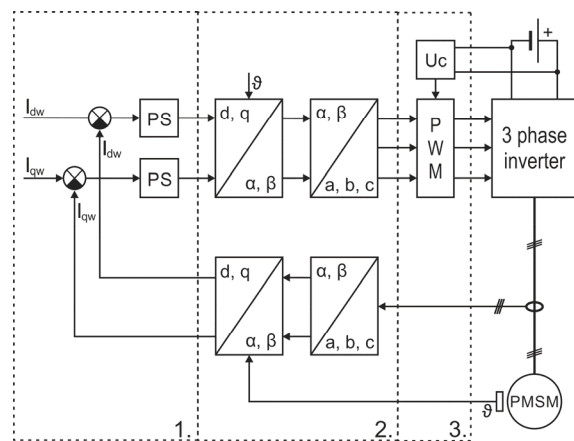


Figure 4. Field-oriented control for permanent magnet synchronous motor

### A. Transformations

FOC uses Park and Clarke transformation to convert a 3-phase system to d, q rotating reference frame.

1) Transformation to the  $\alpha, \beta$

Clarke's transformation converts a 3-phase AC frame  $I_a, I_b, I_c$  to a 2-phase reference frame  $I_\alpha, I_\beta$  with use of equations (1) and (2).

$$I_\alpha = \frac{2}{3}I_a - \frac{1}{3}(I_b - I_c) \quad (1)$$

$$I_\beta = \frac{2}{\sqrt{3}}(I_b - I_c) \quad (2)$$

2) Transformation to the d, q

This transformation describes the relationship between stationary reference frame  $\alpha, \beta$  and the d, q rotating reference frame. These two frames are offset by an  $\vartheta$  angle, which indicates the absolute angle of rotation between the stator axis and the rotor axis. This transformation gives us the relationships described by equations (3) for  $I_d$  and (4) for  $I_q$  respectively.

$$I_d = I_\alpha \cos(\vartheta) + I_\beta \sin(\vartheta) \quad (3)$$

$$I_q = I_\beta \cos(\vartheta) - I_\alpha \sin(\vartheta) \quad (4)$$

3) Back transformation to the  $\alpha, \beta$

The back transformation converts the modulation voltage output from the controllers to a stationary modulation voltage according to equations (5) and (6).

$$U_\alpha = U_d \cos(\vartheta) - U_q \sin(\vartheta) \quad (5)$$

$$U_\beta = U_q \cos(\vartheta) + U_d \sin(\vartheta) \quad (6)$$

4) Inverse transformation to the 3-phase system

The inverse transformation converts the modulation voltage exiting the Park back transform into a 3-phase modulation voltage. The following applies to the reverse transformation:

$$U_a = U_\alpha \quad (7)$$

$$U_b = \frac{-U_\alpha + \sqrt{3} \cdot U_\beta}{2} \quad (8)$$

$$U_c = \frac{-U_\alpha - \sqrt{3} \cdot U_\beta}{2} \quad (9)$$

### B. PS controller

PS controller is composed of proportional and summation is shown in Figure 5. The input variable is the control deviation  $\varepsilon_{(t)}$ , which is the result of subtracting the actual value from the desired value. The proportional term (P) is actually an amplifying element that amplifies the control deviation by the constant  $K_p$ . A summation element (S) is an integration component used in discrete systems. Main goal of (S) term is to eliminate permanent control deviation, which the proportional component is not able to compensate fully to zero. The output of the controller is an action variable used for the intervention of the system: In this case it is the voltage  $U_d$  or  $U_q$ .

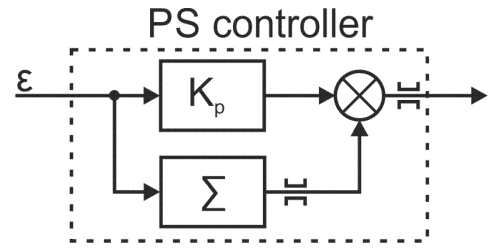


Figure 5. Proportional summation controller

### C. Control algorithm

The control algorithm is programmed to initialize all peripherals when the power is turned on. Initially, all GPIOs are set to inputs with pull-up enabled. This is followed by initialization of PWM, ADC, eCAP, and other peripherals in use, together with the change of GPIO to the desired mode of each connected peripheral. When initialization is complete, the program enters an infinite loop in which execute non-critical tasks. This part of code is responsible for power output control (used for front and rear lights, relay etc.), LED signalization and communications (CAN, RS-485). On the other hand, control loop itself runs in interrupt routine (ISR) as it is required to run it with precise timing and real-time priority. Timing of ISR is derived from PWM carrier frequency of 20 kHz which leads to sampling period of 50 us.

## IV. TEST RESULTS

All measurements were performed on 24V / 10A power supply. To validate hardware itself and also control algorithm implementation, initial measurements were made on compact control unit. Parameters of power supply were sufficient to perform basic testing and tuning of hardware and software. However, it does not allow us to do load tests of the control unit, converter and motor.

Figure 6 shows behavior of absolute position measurement. It can be seen that motor has four pole-pairs (electrical speed four times higher than mechanical). Result shown as CH4 is then used in control loop as theta.

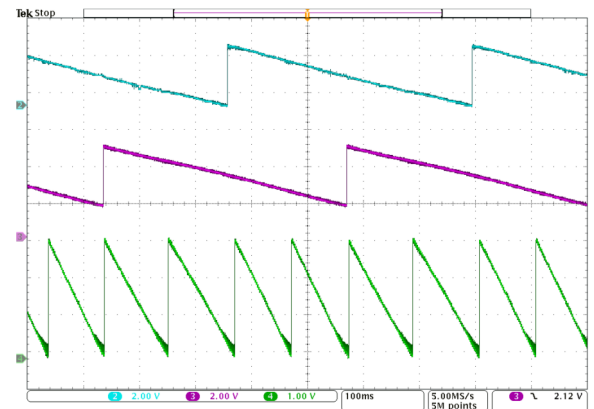


Figure 6. Shaft angle of rotation, CH2 (light blue) - Shaft angle of rotation converted to fixed point ( $0 - 8\pi$ )  $5\pi / \text{div}$ , CH3 (purple) - Shaft angle of rotation from position sensor ( $0 - 2\pi$ )  $1.5\pi / \text{div}$ , CH4 (green) - Shaft angle used in transformations ( $0 - 2\pi$ )  $0.65\pi / \text{div}$



Figure 7 shows the current waveforms in the individual phases of the motor. The motor is unloaded and in steady-state. Variable current amplitude is caused by variable rotor friction. This variable rotor friction has a frequency like one mechanical rotation of the motor. Therefore, it is assumed that this variable amplitude current will be smoothed when the motor will be loaded and will be powered by nominal voltage.

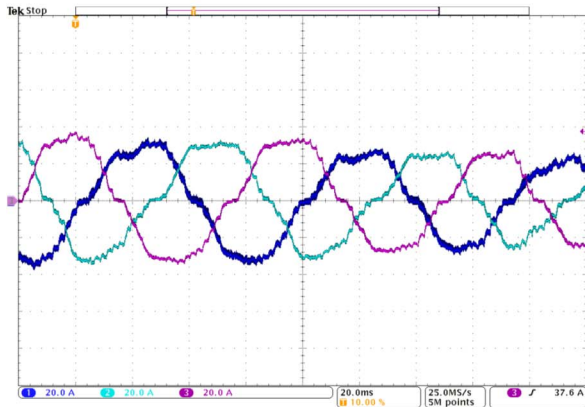


Figure 7. Motor running at current demand  $I_{qw} = 40$ , CH1 (dark blue) - phase current at 20A / div, CH2 (light blue) - phase current at 20A / div, CH3 (purple) - phase current w 20A / div

Figure 8 shows the start of the motor when  $I_{qw} = 40$ . It can be seen from the figure that the motor does not start up until the modulating voltage  $U_q$  (light blue) is sufficiently high.

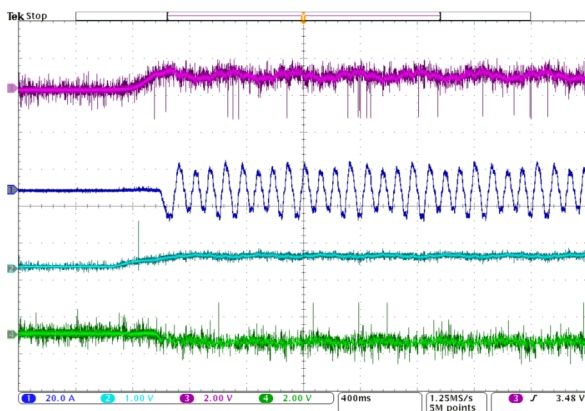


Figure 8. Start for step change of current requirement  $I_q$  from 0 to 40, CH1 (dark blue) - phase current W 20A/div, CH2 (light blue) - modulation voltage  $U_q$  20V/div, CH3 (purple) - current  $I_q$  30A/div (2V/div), CH4 (green) - current  $I_d$  30A/div (2V/div)

## V. CONCLUSION

The developed compact control unit in Figure 9 and implemented algorithms were successfully tested with target motor. However just basic functionality tests were performed.

Next steps will be assembly control unit with go-kart and perform load test together with test of communications and auxiliary peripherals (lights, pedals etc.).



Figure 9. Control board with 3-phase inverter

## ACKNOWLEDGMENT

This project has been supported by the Ministry of Education, Youth and Sports of the Czech Republic under the project OP VVV Electrical Engineering Technologies with High-Level of Embedded Intelligence CZ.02.1.01/0.0/0.0/18\_069/0009855 and under project SGS-2018-009.

## REFERENCES

- [1] C. Cardoso, J. Ferreira, V. Alves and R. E. Araujo, "The design and implementation of an electric go-kart for education in motor control," International Symposium on Power Electronics, Electrical Drives, Automation and Motion, 2006. SPEEDAM 2006., Taormina, 2006, pp. 1489-1494.
- [2] W. O. Avelino, F. S. Garcia, A. A. Ferreira and J. A. Pomilio, "Electric go-kart with battery-ultracapacitor hybrid energy storage system," 2013 IEEE Transportation Electrification Conference and Expo (ITEC), Detroit, MI, 2013, pp. 1-6.
- [3] J. Stepanek, B. Bednar, L. Streit and L. Elis, "Electric kart "FeLiS" with LiFeYPO<sub>4</sub> batteries," 2013 International Conference on Clean Electrical Power (ICCEP), Alghero, 2013, pp. 151-154.
- [4] "TMS320F28335," TMS320F28335 C2000™ 32-bit MCU with 150 MIPS, FPU, 512 KB Flash, EMIF, 12b ADC | TI.com. [Online]. Available: <http://www.ti.com/product/TMS320F28335>. [Accessed: 08-Apr-2020].
- [5] "TLC555," TLC555 2.1-MHz, 250- $\mu$ A, Low-Power Timer | TI.com. [Online]. Available: <http://www.ti.com/product/TLC555>. [Accessed: 08-Apr-2020].
- [6] Z. Peroutka, "Design considerations for sensorless control of PMSM drive based on extended Kalman filter," 2005 European Conference on Power Electronics and Applications, Dresden, 2005, pp. 10 pp.-P.10.
- [7] O. Saadaoui, A. Khlaief, M. Abassi, A. Chaari and M. Boussak, "Position sensorless vector control of PMSM drives based on SMO," 2015 16th International Conference on Sciences and Techniques of Automatic Control and Computer Engineering (STA), Monastir, 2015, pp. 545-550.
- [8] "AS5040 Rotary Sensor," ams. [Online]. Available: <https://ams.com/as5040>. [Accessed: 08-Apr-2020].
- [9] F. Yusivar, N. Hidayat, R. Gunawan and A. Halim, "Implementation of field oriented control for permanent magnet synchronous motor," 2014 International Conference on Electrical Engineering and Computer Science (ICEECS), Kuta, 2014, pp. 359-362.
- [10] A. Samar, P. Saedin, A. I. Tajudin and N. Adni, "The implementation of Field Oriented Control for PMSM drive based on TMS320F2808 DSP controller," 2012 IEEE International Conference on Control System, Computing and Engineering, Penang, 2012, pp. 612-616.
- [11] Z. Peroutka, K. Zeman, F. Kros and F. Kosta, "Control of permanent magnet synchronous machine wheel drive for low-floor tram," 2009 13th European Conference on Power Electronics and Applications, Barcelona, 2009, pp. 1-9.